SESSION 1. SOLAR ASTROPHYSICS

https://doi.org/10.1017/S0252921100085146 Published online by Cambridge University Press

THE SOFT X-RAY AND EUV SPECTRA OF SOLAR FLARES.

K.Nishi and K.Tanaka
Tokyo Astronomical Observatory, University of Tokyo
Mitaka Tokyo Japan

HINOTORI

The Japanese solar maximum satellite HINOTORI was launched on 21 February 1981, and so far 720 Solar flares were detected including many large flares; the largest observed was a X12 class flare occurred on June 6, 1982. Unfortunately, the data recorder malfunctioned in June, 1982, since then the real time basis observation has been possible to continue. The general introductory explanation and some important results were already published in some proceedings(1,2,3), therefore we would like to focus on presenting some new results of the Soft X-ray spectra obtained by the spectrometers rather than on talking a review.

The Soft X-ray crystal spectrometers (SOX) measure spectral features around 1.85A emitted from highly ionized iron ions with two different spectral ranges and resolutions; low (SOX-1;1.72-1.99A; 2.5mA) high (SOX-2; 1.83-1.89A; 0.15mA), with temporal resultion of 8-10 seconds. They were newly designed Bragg type spectrometers for the spin stabilized satellite. The wavelength scan is made automatically by the spin without moving any parts of the spectrometers. (Tanaka et al., 1978) The idea to use the attitude of space vehicle is our traditional method applied for the Solar observation from rockets (Nishi, 1973,1975). Another instrument for Flare Monitor (FLM) was used to measure Soft X-ray spectrum in the energy range of 1.5-30 kev. The detector is a gas-sealed scintillation proportional counter, and the energy resulution is 10.5% at 5.9 kev nearly twice superior to ordinary proportional counters. An example of spectra obtained by the crystal spectrometers is shown in the figure 1. The high resolution spectra (lower) cover lines from FeXXV to FeXXIII, and low resolution spectra (upper) show lines from FeXIX to FeXXVI, $K\alpha$ and $K\beta$. The FeXXVI lines are resolved into four peaks: 1.778A($L\alpha_1$), 1.784A($L\alpha_2$), 1.789A and 1.792A. The latter two peaks are from the satellite lines(FeXXV) associated with FeXXVI. Their relative intensities are various from flare to flare. An example of time behaviors of various lines and plasma parameters such as electron temperature(Te), ionization temperature(Tz), dI(total iron lines intensity)/dt, and Hard X-ray seen in one of the published papers (Tanaka et al.,1982). There are many types of variations, but some common characteristics can be summarized as follows. At the initial phase of the flare the lines are broad(200km/s) and have blue shift component (400km/s), and the blue-shifted components show limb weakening. The line width of unshifted components monotonically decreases from the start to the end of flare, which suggests that large non-thermal broadening (turbulent motion) occurred in the flaring plasma at the beginning of flare. For the analysis of velocity shift a method of line

https://doi.org/10.1017/S0252921100085146 Published online by Cambridge University Press

profile fitting to synthesized spectra by using the atomic parameters from Dubau et al. (1981) and Bely-Dubau et al. (1982a, b) is used. In rare cases lines with red shift component are also found and is shown in the figure 2. In the very initial phase of the biggest flare observed by HINOTORI a double-peaked w line profile was detected in low resolution spectra of two consecutive scans made with 10sec. interval, and the separation corresponds to 300km/s. (Fig.3) If the blue shift is interpreted as rising motion of heated plasma from denser atmosphere which is heated by electron beam or heat conduction, and if the rising plasmas are confined in the lower portion of the coronal loops, then the increse of total electron number of stationary hot plasma is explained by supply of input electron number from the blue-shifted plasma. An analysis is now under progress comparing with the filtergrams of H_α and D_3 emission and the X-ray image by K.Tanaka and others.

The electron temperatures (Te) for FeXXV are derived from the well-known method of using the line intensity ratio of dielectronic satellite (j) to resonance (w) shown by Gabriel et al.(1972); Doschek et al.(1980) or the spectal line profile fitting method, and their values are quite consistent with each other. Te for FeXXVI plasma are derived from the synthesized spectra calculated from the atomic data by Dubau et al, (1981) with the crystal resolution, and we can safely assumed that the fitting accuracy is within ± 2 million K at most. In the figure 4 we see that Te from the FeXXVI and FeXXV spectra are different significantly. One of the most important characteristic of our instruments is that we can obtain FeXXVI spectra, and the more intensive FeXXVI spectra were observed the more clear the difference appeared. The time behavior of FeXXVI line in some flares is quite similar to the Hard X-ray intensity but different from FeXXV and lower ionization stage lines; it reachs its maximum about 1 minute before FeXXV lines reach the peak. According to the characteristics and time behaivors of hot thermal component derived from FeXXVI lines as shown above, flares could be classified into two categories; Type A and B. (Tanaka et al. 1983 for Type C see Tsuneta et al. 1984) In Type A flare, the lowest energy of hard X-ray shows no spiky compoments and its time behavior is quite similar to FeXXVI lines. The FeXXVI spectra show the existence of hot thermal component with Te $30\text{-}40 \times 10^6$K, and the obtained emission measure Ne^2V is 10^{49} $-10^{50}/cm^3$. These flares are very compact and short-lived in the low corona from the X-ray telescope (SXT), then electron density can be derived as 10^{11-12} $/cm^3$, since it is safely assumed that emitting regions of FeXXVI and hard X-ray are overlapped. Type B flares show quite different characteristics at the beginning. While hard X-ray time profiles consist of spikes to the lowest channel, FeXXVI lines behave differently except for later phases. Most valuable characteristics could be the similarity of time profile of dI/dt(I:total iron line emission) to that of the hard X-ray bursts. This fact suggests that production of thermal component (Te$\sim$20

https://doi.org/10.1017/S0252921100085146 Published online by Cambridge University Press

$\times 10^6$ K) is closely associated with the occurrence of hard X-ray spike bursts. Continum observations by FLM show also this characteristics (Watanabe et al. 1983). The difference between Type A and Type B may originate from the difference of relative importance of two components, i.e. in Type A flares contribution of hot thermal component dominates spike component, while in Type B flares, hot thermal component contributes somewhat only in the decay phase.

For the ionization balance between FeXXIV and FeXXV Te and Tz are derived from j/w and q/w (q; inner shell excitation line) respectively, and the observed data are almost consistent with the Shull and Van Steenberg (1982) computations. (F.Moriyama, 1984) But observed FeXXVI/FeXXV values derived from the values of Lα/w and z/w are quite different from the theoretical curves (Fig. 5:a,b). On the other hand at the Maximum phase of type A flares the ratios show nearly equilibrium if Te derived from FeXXVI line profile fitting is referred (Fig. 5,c). From the time profile of Te(XXVI) and Te(XXV) we see that Te(XXVI)$>$ Te(XXV) at the maximum phase (Fig. 5,d) but Te(XXVI)$\gtrsim$ Te(XXV) at the later phase (Fig. 6). Does the discrepancy depend on the physical situation of the flare plasmas or on the theoretical calculations of atomic parameters? The differential emission measure calculations are also not able to solve the problem. (Akita, 1984) The exceptionally intense iron Kα emissions associate with hard X-ray burst were observed by the spectrometer. High resolution continuum spectra from 1.5 to 12.5kev and hard X-ray spectra from 18 to 400kev of the flares were obtained by the gas scintillation counter and the scintillation counter. They show remarkable power-law photon distribution extending from below 10kev to above 100 kev in the early phase of the flares. The intense Kα emission is attributed to fluorescence of photospheric neutral iron by the power-law X-ray flux that extends down to the K-shell ionization threshold at 7.1 kev. On the other hand, the gradually increasing Kα emission after the decay of the hard X-ray burst can be explained by fluorescence due to the X-ray flux of thermal origin. (Tanaka et al. 1984)

As SOX has two independent crystals with different phase angles, it provides a new technique for measuring linear polarization of iron emission line (Akita et al. 1983). The upper limit of averaged polarization degree was determined as about 4%.

From the FLM data we can derive Te and EM (Emission measure) by adopting a proper modeling. From time behavior Te v.s. EM in a flare we see that EM increases as Te increases like heating due to adiatic compression. However, EM reaches maximum after Te maximum, and then EM remains though Te decreases. If the dominant process of this phase is radiative cooling, electron density is estimated to be $5 \times 10^{11}/cm^3$ (Watanabe et al. 1982).

TENMA

The second X-ray astronomy satellite, nickmamed TENMA (a Japanese for Pegasus) was put into orbit sucessfully on

https://doi.org/10.1017/S0252921100085146 Published online by Cambridge University Press

20 February 1983. TENMA carries four scientific instruments; GSPC (gas scintillation proportional counter), XFC (X-ray Focusing Concentrator), TSM (Transient Source Monitor), and GBD/RBM(Gamma-ray Burst Detector/Radiation Belt Monitor). The main instrument is GSPC consisting of ten modular units, two of which are equipped with modulation collimators. It is the same type dector as FLM on HINOTORI, and provides a powerful capability for the spectroscopic study of various categories of cosmic X-ray sources in 1-60 kev. Its large effective area, about 640cm^2 for eight GSPCs, ensures a sensitivity down to 1/2000 the Crab Nebula flux, making the observations of various extragalatic sources possible. Its capability is illustrated by the X-ray spectrum of a supernova Cas A compared with one of the solar flares (Fig. 7). Since the launch, TENMA has been yielding many significant results (Y.Tanaka 1983), but we would like to show two of them obtained by GSPC.

The spectra from X-ray pulsars (mostly composed of a massive star and a magnetized neutron star) often exhibit a K-emission line at about 6.4 kev as well as iron K absorption edge around 7.1 kev (Fig. 8), indicating that there is a relatively cold matter around the X-ray emitting neutron star. Another example is the discovery of an X-ray absorption line at about 4.1 kev in X-ray burst spectra from 4U 1636-53. (Fig. 9) This may be interpreated as the iron absorption line, redshifted due to a high gravity of the neutron star surface. These results lead to direct measurements of the mass and size of the neutron star.

Rocket observation of the EUV images of a flare and active regions.

Heliograms of a flare and active regions were obtained in EUV emission lines such as CIII 970A, NeVIII 770A, HI Ly$_\beta$, and hydrogen Lyman continua with a spatial resolution of 10 seconds of arc and pointing accuracy of about 0.5 seconds of arc by a Japanese sounding rocket S520-5CN. The instrument was composed of a 10cm Cassegrain telescope (F/15), a 50cm stigmatic spectrograph, and a two dimensional microchannel plate. The second mirror of the telescope was used for the fine pointing and raster scan. The entrance slit of the spectrograph and the group of slits to separate emission lines and hydrogen continua were set on the Rowland circle, and the microchannel plate was set on the spatial (vertical) foci. The rocket was launched on Sept. 6 1982, at 02h00m00s UT from the Kagoshima Space Center, reaching maximum hight of 237 km at 246s. after firing. Very fortunately an 1B flare was occuring 01h52m-02h22m UT (Max. 01h53m) at N14 and E12. From the obtained data some physical parameters such as Te, Tb, and thickness of emitting layer for quite region, active region, and flare were derived (Hirayama et al. 1984).

REFERENCES

(1) Proceedings of HINOTORI symposium on Solar Flares; (Tokyo, 27-29 January, 1982) published by ISAS, May(1982)

https://doi.org/10.1017/S0252921100085146 Published online by Cambridge University Press

(2) Proceedings of US-Japan Seminor on Recent Advance in Understanding of Solar Flares, Solar Phys., 86, Nos. 1,2(1983)
(3) Proceedings of the Japan-France Seminor on Active Phenomena in the Outer Atmosphere of the Sun and Stars, (Paris, 3-7 Octover 1983) publiched by CNRS, (1984)
Akita, K., Tanaka, K., and Watanabe, T. 1983, Solar Phys., 86, 101.
Akita, K., 1984, private communication.
Bely-Dubau, F., Dubau, J., Faucher, P., and Gabriel, A. H. 1982a, M. N. R. A. S., 198, 239.
Bely-Dubau, F. et al. 1982b, M. N. R. A. S., 201, 1155.
Doschek, G.A., Feldmann, U., Kreplin, R.W., and Cohen, L., 1980 Astrophys. J., 239, 725
Dubau, J. et al. 1981, M. N. R. A. S., 195, 705.
Gabriel, A.H. 1972, M. N. R. A. S., 160, 99.
Hirayama, T., et al., 1984; submitted to Solar Phys.
Moriyama, F., 1984; private communication.
Nishi, K., 1973, Solar Phys., 33, 23.
Nishi, K., 1975, Solar Phys., 42, 37.
Shull, J.M., and Van Steenberg, M., 1982, Astrophys. J., Sup. Ser., 48, 95.
Tanaka, K. and Nishi, K., 1978, Jap. J. Applied Phys. 17, Suppl. 17-2, 461.
Tanaka, K., Watanabe, T., Nishi, K. and Akita, K., 1982, Astrophys. J. Letters, 254, L59.
Tanaka, K., Nitta, N., Akita, K., and Watanabe, T., 1983, Solar Phys., 86, 91.
Tanaka et al., 1984, Astrophys. J. July 15 issue.
Tanaka, Y., 1983, ISAS Research Note No. 240.
Tsuneta, S., Takakura, T., Nitta, N., Ohki, K., Tanaka, K., Makishima. K., Murakami, T., Oda, M., Ogawara, Y., Kondo, I., 1984, Astrophys. J., 280, 887.
Watanabe, T., Tanaka, K., and Matsuoka, M., 1982, p.14; HINITORI Symp. on Solar Flares; published by ISAS.
Watanabe, T., Tanaka, K., Akita, K., and Nitta, N., 1983, Solar Phys., 86, 107.

FIGURE CAPTIONS

Fig.1 An example of Soft X-ray spectra; upper is low resolution and lower is high resolution.
Fig.2 An example of red shift component. The spectra are fitted to theoretically synthesized spectra (dash line).
Fig.3 An example of double-peaked w line profiles; June 6 1982 flare, two successive data of 16h30m31s-41s and 16h30m41s-50s show double peak at 1.85Å.
Fig.4 The existence of two temperature plasmas. upper; when Te (26.9×10^6K) determined by the Fe(XXV) profile fitting is adopted, the observed FeXXVI line profile do not fit to the calculated profile (dashed). lower; when Te (40×10^6K) determined by the Fe(XXVI) line profile fitting is adopted, the observed FeXXV profile

do not fit the calculated one.

Fig.5 (a)H/He derived from Lα/w v.s. Te determined by the FeXXV line profile fitting.
(b)H/He derived from z/w v.s. Te determined by the FeXXV line profile fitting.
(c)H/He derived from Lα/w v.s. Te determined by the FeXXI line profile fitting.
(d)Te(FeXXVI) v.s. Te(FeXXV) at the maximum phase.
(from Tanaka, K., and Akita, k., 1984 in preparation.)

Fig.6 Time profile of plasma parameters. (from Tanaka, K., Ohki, K., and Zirin, H., 1984, to be submitted to Astrophys. J.).

Fig.7 Comparison of Soft X-ray spectra of a solar flare observed by FLM on HINOTORI(left) and a typical young supernova remnant Cas A observed with GSPC on TENMA (right). K-emmission lines from various elements, including silicon, sulpher, argon, calcium, and iron are clearly resolved. (from SPACE RESEARCH IN JAPAN 1984, National report submitted to the 25 Plenary Meeting of the ICSU Committee on Space Research)

Fig.8 X-ray spectra of X-ray pulsars some times show strongly absorbed features. This is an example observed from Vela X-1 by the TENMA GSPC. An intense iron fluoresence line emission at about 6.4kev is seen, as well as a deep absorption edge by cold iron at about 7.1 kev. (from SPACE RESEARCH IN JAPAN 1984)

Fig.9 An X-ray absorption line was discovered with the TENMA GSPC in X-ray burst spectra from 4U 1636-53. This line, at about 4.1kev, is tentatively identified with the iron K-line, orginally at 6.4kev, redshifted due to an immense gravity on the neutron star surface. (from SPACE RESEARCH IN JAPAN 1984)

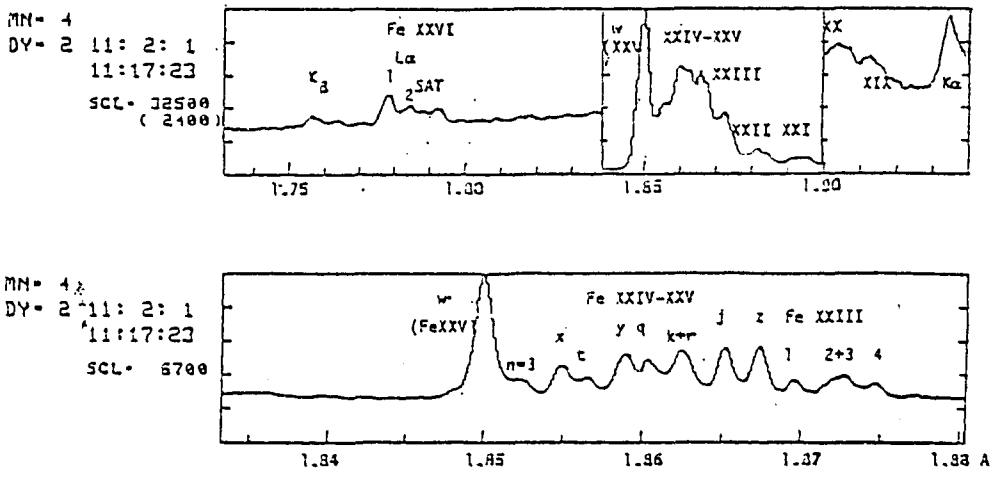

Fig.1

https://doi.org/10.1017/S0252921100085146 Published online by Cambridge University Press

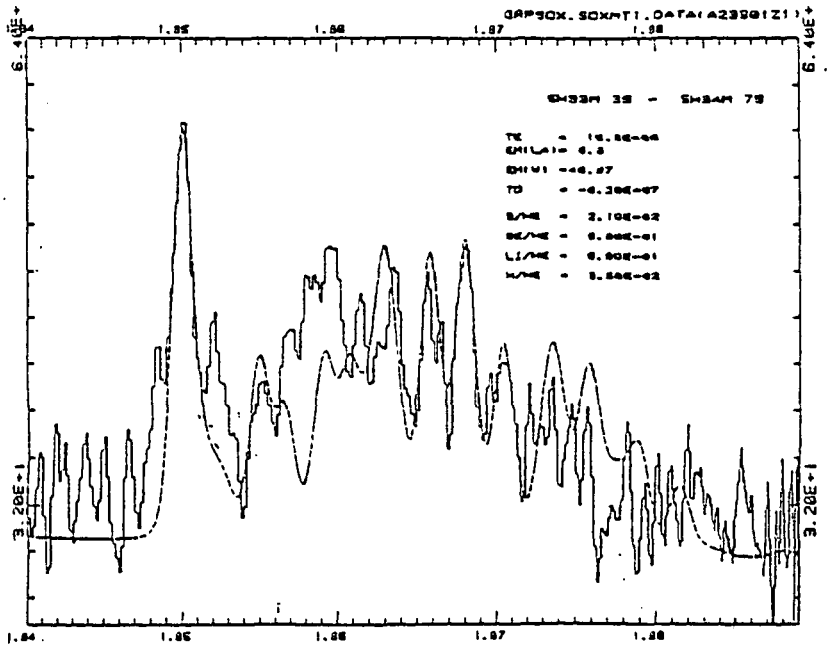

Fig.2

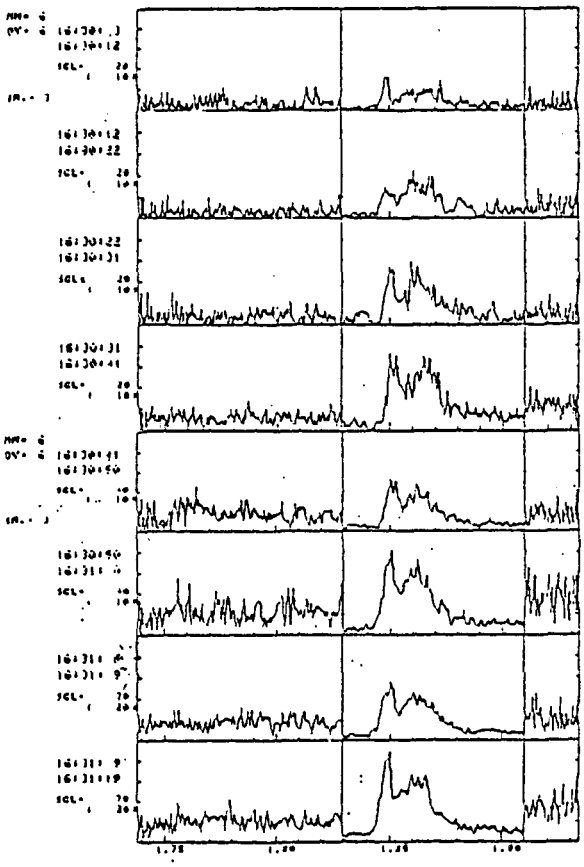

Fig.3

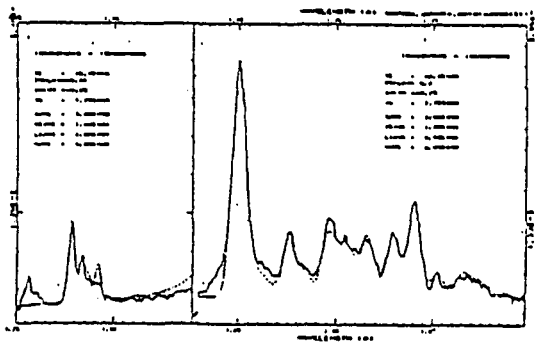

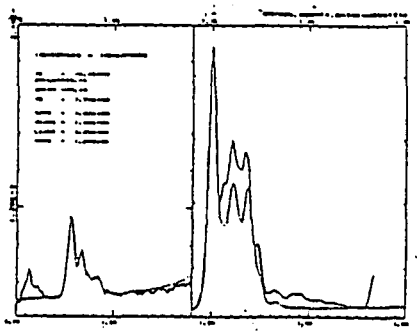

Fig.4

https://doi.org/10.1017/S0252921100085146 Published online by Cambridge University Press

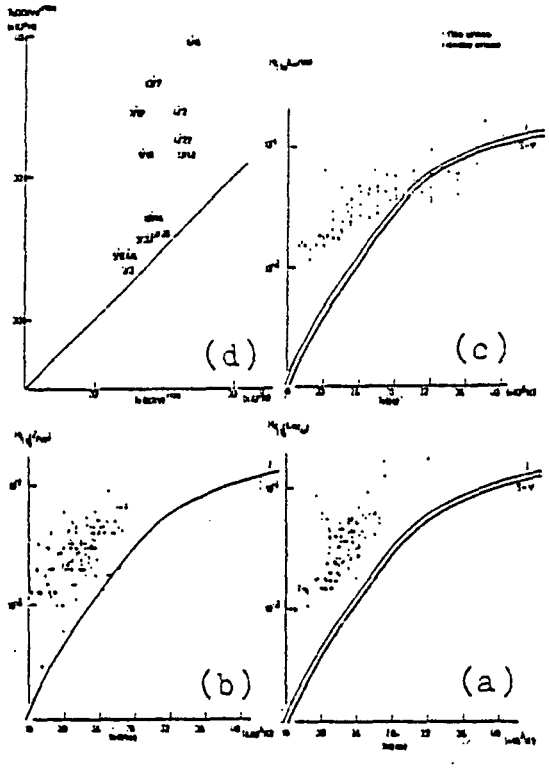

Fig.5

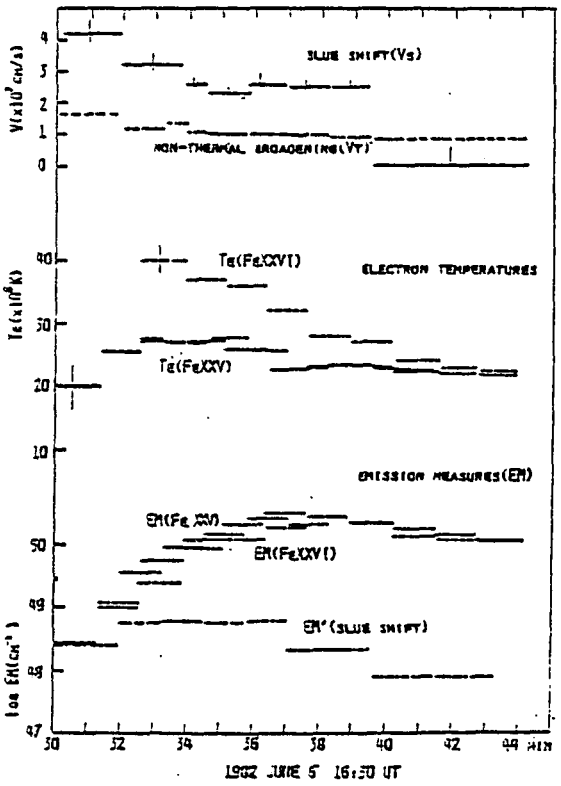

Fig.6

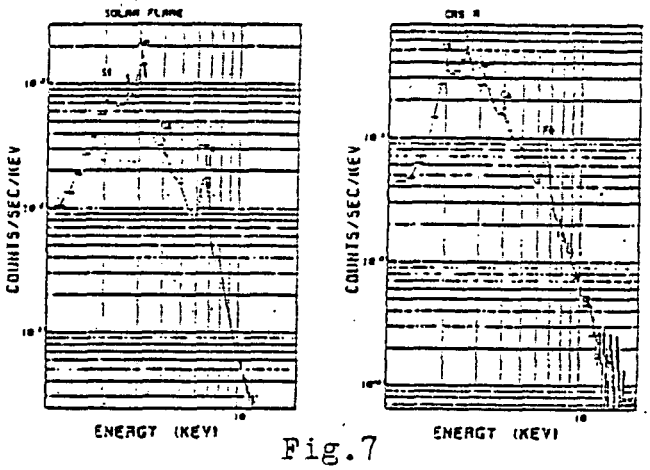

Fig.7

Fig.8

Fig.9

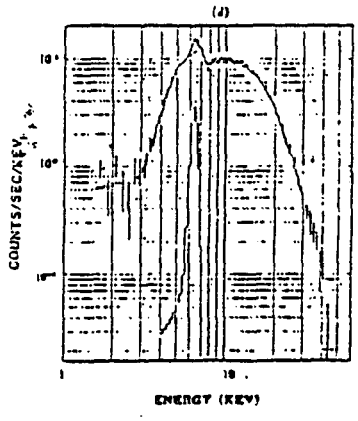

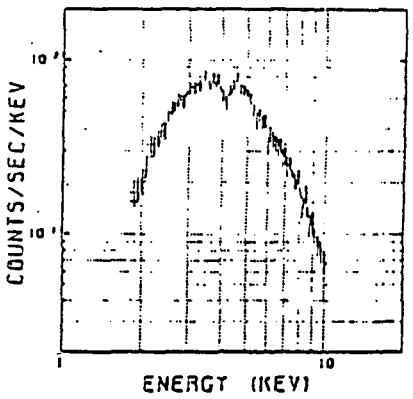

https://doi.org/10.1017/S0252921100085146 Published online by Cambridge University Press